High Yield of Germanium Nanocrystals Synthesized from Germanium Diiodide in Solution

Xianmao Lu, Brian A. Korgel,* and Keith P. Johnston*

Department of Chemical Engineering, Texas Materials Institute, and Center for Nano- and Molecular Science and Technology, The University of Texas at Austin, Austin, Texas 78712

Received July 20, 2005. Revised Manuscript Received August 25, 2005

High chemical yields, up to 73%, were achieved for germanium (Ge) nanocrystals synthesized in solution with germanium diiodide (GeI_2) and $LiAlH_4$ as a reducing agent in tri-*n*-octylphosphine (TOP) or tri-*n*-butylphosphine (TBP). Ge nanocrystals were characterized by transmission electron microscopy (TEM), energy-dispersive X-ray spectroscopy (EDS), X-ray diffraction (XRD), Fourier transform infrared (FTIR) spectroscopy, and X-ray photoelectron spectroscopy (XPS). Reactions in TOP at 300 °C yielded Ge nanocrystals with moderate size polydispersity and good crystallinity with average diameters that could be manipulated by varying the precursor concentration from ∼3 to ∼11 nm. High chemical yields are enabled by the high reactivity of GeI_2, high GeI_2 solubility in alkyl phosphines, and relatively mild reaction temperature, which minimizes byproduct formation and solvent degradation. Compared to reactions carried out in TOP with the same concentration of GeI_2, nanocrystals synthesized in TBP at 240 °C exhibit larger size and broader size distribution. The presence of alkyl groups in the FTIR spectra, the small and controllable particle diameters, and a lack of significant Ge oxidation revealed by XPS indicate that the nanocrystals were chemically passivated with an organic layer.

Introduction

Semiconductor nanocrystals exhibit size-tunable optical and electronic properties that are of interest in solid-state lighting, sensors, and other electronic and optoelectronic devices.[1,2] Solution-phase methods have been developed to produce a wide range of materials, including metal,[3−5] and Group II−VI,[6] III−V,[7] and IV[8] semiconductor nanocrystals by reacting precursors in the presence of organic capping ligands. For Ge nanocrystals, it has been challenging to identify appropriate precursors that readily decompose in the presence of organic ligands and sustain controlled crystalline particle growth. Many synthetic approaches have been explored, including $GeCl_4$ reduction with reducing agents such as NaK alloy[9] and sodium or lithium naphthalenide,[10] reduction of $GeCl_4$ in inverse micelles combined with separation using HPLC,[11] metathesis reactions of NaGe, KGe, or Mg_2Ge with $GeCl_4$,[12−15] thermally initiated hydrogermylation of GeI_4,[16] organogermane thermolysis (for example, tetraethylgermane (TEG) and diphenylgermane (DPG)) in high-temperature organic solvent[17] or in supercritical solvents,[18−20] thermal reduction of $Ge[N(SiMe_3)_2]_2$ in a noncoordinating solvent,[21] and reduction of $GeCl_4$ in inverse micelles to make Ge nanocubes.[22] These methods have not been able to achieve simultaneously a high yield of crystalline well-passivated Ge nanocrystals with controlled size and low polydispersity, due to the limitations of limited precursor reactivity, particularly for $GeCl_4$; byproduct formation, for example, from organogermanes; and poor ligand stabilization.

Here, we report the synthesis of Ge nanocrystals by reduction of germanium diiodide (GeI_2) with $LiAlH_4$ in

* Corresponding authors. Telephone: 512-471-5633 (B.A.K.); 512-471-4617 (K.P.J.). Fax: 512-471-7060 (B.A.K.); 512-471-7060 (K.P.J.). E-mail: korgel@che.utexas.edu (B.A.K.); kpj@che.utexas.edu (K.P.J.).

(1) Heath, J. R. *Chem. Soc. Rev.* **1998**, *27*, 65.
(2) Alivisatos, A. P. *Science* **1996**, *271*, 933.
(3) Sigman, M. B., Jr.; Saunders, A. E.; Korgel, B. A. *Langmuir* **2004**, *20*, 978.
(4) Saunders, A. E.; Sigman, M. B., Jr.; Korgel, B. A. *J. Phys. Chem. B* **2004**, *108*, 193.
(5) Son, S. U.; Jang, Y.; Yoon, K. Y.; Kang, E.; Hyeon, T. *Nano Lett.* **2004**, *4*, 1147.
(6) Murray, C. B.; Norris, D. J.; Bawendi, M. G. *J. Am. Chem. Soc.* **1993**, *115*, 8706.
(7) Stowell, C. A.; Wiacek, R. J.; Saunders: A. E.; Korgel, B. A. *Nano Lett.* **2003**, *3*, 1441.
(8) Holmes, J. D.; Ziegler, K. J.; Doty, R. C.; Pell, L. E.; Johnston, K. P.; Korgel, B. A. *J. Am. Chem. Soc.* **2001**, *123*, 3743.
(9) Heath, J. R.; Shiang, J. J.; Alivisatos, A. P. *J. Chem. Phys.* **1994**, *101*, 1607.
(10) Kornowski, A.; Giersig, M.; Vogel, R.; Chemseddine, A.; Weller, H. *Adv. Mater.* **1993**, *5*, 634.
(11) Wilcoxon, J. P.; Provencio, P. P.; Samara, G. A. *Phys. Rev. B* **2001**, *64*, 035417.
(12) Taylor, B. R.; Kauzlarich, S. M.; Delgado, G. R.; Lee, H. W. H. *Chem. Mater.* **1999**, *11*, 2493.
(13) Tanke, R. S.; Kauzlarich, S. M.; Patten, T. E.; Pettigrew, K. A.; Murphy, D. L.; Thompson, M. E.; Lee, H. W. H. *Chem. Mater.* **2003**, *15*, 1682.
(14) Taylor, B. R.; Fox, G. A.; Hope-Weeks, L. J.; Maxwell, R. S.; Kauzlarich, S. M.; Lee, H. W. H. *Mater. Sci. Eng., B*− **2002**, *96*, 90−93.
(15) Taylor, B. R.; Kauzlarich, S. M.; Lee, H. W. H.; Delgado, G. R. *Chem. Mater.* **1998**, *10*, 22−24.
(16) Fok, E.; Shih, M.; Meldrum, A.; Veinot, J. G. C. *Chem. Commun.* **2004**, 386.
(17) Gerion, D.; Zaitseva, N.; Saw, C.; Casula, M. F.; Fakra, S.; Van Buuren, T.; Galli, G. *Nano Lett.* **2004**, *4*, 597.
(18) Lu, X.; Ziegler, K. J.; Ghezelbash, A.; Johnston, K. P.; Korgel, B. A. *Nano Lett.* **2004**, *4*, 969.
(19) Myung, N.; Lu, X.; Johnston, K. P.; Bard, A. J. *Nano Lett.* **2004**, *4*, 183.
(20) Lu, X.; Korgel, B. A.; Johnston, K. P. *Nanotechnology* **2005**, *16*, S389.
(21) Gerung, H.; Bunge, S. D.; Boyle, T. J.; Brinker, C. J.; Han, S. M. *Chem. Commun.* **2005**, 1914.
(22) Wang, W. Z.; Huang, J. Y.; Ren, Z. F. *Langmuir* **2005**, *21*, 751−754.

10.1021/cm0515956 CCC: $30.25
Published on Web 11/15/2005

coordinating solvents, tri-*n*-octylphosphine (TOP) or tri-*n*-butylphospine (TBP), with high chemical yields. GeI_2 disproportionates to Ge and GeI_4 at ~330 °C, and this reaction has been used to grow Ge films by chemical vapor deposition at higher temperatures.[23,24] Wu et al. recently synthesized single-crystalline Ge nanowires from GeI_2 by a vapor transport method at temperatures about 1000 °C.[25] When mixed with alkyl phosphines R_3P, such as TOP and TBP, GeI_2 and R_3P react to form adducts of $(GeI_2)\cdot R_3P$.[26] The TOP·(GeI_2) and TBP·(GeI_2) complexes are soluble in organic solvents, offering the opportunity for Ge synthesis in solution under mild reaction temperature of 300 °C and atmospheric pressure. The goal was to achieve a high chemical yield of Ge nanocrystals by taking advantage of the high reactivity of GeI_2 and high GeI_2 solubility in alkyl phosphines and to use mild reaction temperatures to minimize solvent degradation byproducts. The coordinating solvents (i.e., TOP and TBP) control the rate of precursor decomposition and serve as capping ligands to prevent particle aggregation, leading to relatively monodisperse nanocrystals. Preliminary experiments performed by heating GeI_2 in TOP at 330 °C gave observable quantities of Ge nanocrystals. However, the nanocrystal surfaces were heavily oxidized, and the yield was low. The addition of $LiAlH_4$ as a reducing agent was found to prevent surface oxidation and increase the reaction yield significantly, resulting in chemical yields of up to 73%. The method of addition of the precursor and $LiAlH_4$ and the temperature profile were designed to produce high nucleation rates and to control the particle size. The Ge nanocrystals were crystalline with moderate polydispersity. Coarse size control can be achieved by varying the precursor concentration, with higher GeI_2 concentrations giving larger particles. In addition to the high yield of Ge nanocrystals, this report also describes the effect of precursor concentration and different solvents on the nanocrystal size and the growth mechanism. The competition between growth by condensation and aggregation is analyzed on the basis of the moments in the size distribution. The results are compared with previous synthetic methods, which have explored a wide range of temperatures with various types of precursors, reducing agents, stabilizing ligands, and solvents.

Experimental Section

Synthesis. Ge nanocrystals were synthesized under nitrogen in a three-neck flask on a Schlenk line. GeI_2 (Strem Chemicals, packed under argon) were stored in a nitrogen-filled glovebox upon purchase. Both TOP and TBP (Aldrich, technical grade) were degassed through a freeze−pump−thaw technique, and TOP was distilled at 200 °C and 0.3 Torr. TBP and vacuum-distilled TOP were then transferred into the glovebox, and 4 Å molecular sieves were used to absorb the water in the solvents. The precursor solutions were prepared in the glovebox. Amounts of 0.215, 0.43, and 0.86 g of GeI_2 were added to 5 mL of TOP or TBP and stirred for 10 h to form clear yellow solutions with concentrations of 130, 260, and 520 mM, respectively. Amounts of 0.0125, 0.025, and 0.05 g of $LiAlH_4$ (Aldrich) were added to 5 mL of TOP or TBP and also stirred for 10 h to form 65, 130, and 260 mM dispersions. The GeI_2 and $LiAlH_4$ mixtures were loaded separately into 10 mL glass syringes. A 5 mL aliquot of GeI_2 solution was injected into the flask through a rubber septum and heated to 120 °C with stirring, followed by the injection of 5 mL of the corresponding $LiAlH_4$ dispersion. The $LiAlH_4$ concentration was about half that of GeI_2. The introduction of $LiAlH_4$ immediately produced a brown solution. The temperature was raised to 300 °C for reaction in TOP and 240 °C in TBP within 5 min, and the solution gradually turned black in 2 min. After 60 min, the heating mantle was removed and the products were allowed to cool to room temperature. A 10 mL aliquot of acetone was added to the mixture to form a black precipitate containing Ge, and the mixture was centrifuged. The Ge nanocrystals were redispersed in 10 mL of chloroform, reprecipitated with 10 mL of acetone, and centrifuged again at 9000 rpm for 5 min. This purification step was repeated again. A final centrifugation of redispersed nanocrystals in 10 mL of chloroform at 6000 rpm for 5 min resulted in a dark gray solution of Ge nanocrystals and precipitate containing impurities. The Ge nanocrystals were vacuum-dried on a rotary evaporator at room temperature. About 23, 70, and 95 mg of black powder consisting of Ge nanocrystals was obtained after the purification steps for reactions of 130, 260, and 520 mM GeI_2 in TOP corresponding to chemical yields of 48, 73, and 50%, respectively. The nanocrystals readily redisperse in chloroform and toluene.

Materials Characterization. The nanocrystals were characterized by transmission electron microscopy (TEM), energy-dispersive X-ray spectroscopy (EDS), Fourier transform infrared (FTIR) spectroscopy, and X-ray photoelectron spectroscopy (XPS). TEM specimens were prepared by drop-casting dilute dispersions onto 200-mesh copper grids coated with ultrathin carbon film (Ladd Research Co.). Low-resolution TEM (LRTEM) images were obtained with a Philips EM201 TEM operating at 80 kV. High-resolution TEM (HRTEM) was performed on a JEOL 2010F TEM; images were obtained digitally with a GATAN digital photography system. EDS was performed on the JEOL 2010F HRTEM equipped with an Oxford spectrometer. XPS data was acquired using a Physical Electronics XPS 5700 ESCA spectrometer equipped with a monochromatic Al X-ray source (Al Kα, 1.4866 keV) and 11.7 eV path energy by drop-casting 2 mg of nanoparticles from chloroform onto a 1 × 1 cm silicon substrate. X-ray diffraction (XRD) was obtained from ~10 mg nanocrystals deposited by drop-casting on quartz slides (Gem Dugout, State College, PA) with a continuous scan for 5 h at a rate of 12°/min and 0.02°/step using a Bruker-Nonius D8 Advance powder diffractometer with Cu *K*α radiation ($\lambda = 1.54$ Å) and a rotary sample stage (30 rpm). FTIR measurements were performed using a Thermo Mattson Infinity Gold FTIR spectrometer for purified Ge nanocrystals that were drop-cast in air from chloroform onto a KBr IR card (International Crystal Laboratories).

Results

Nanocrystal Synthesis in TOP. Figure 1 shows representative TEM images of Ge nanocrystals made from different GeI_2 concentrations in TOP: 130, 260, and 520 mM. The particles have not been size-selectively precipitated. The samples are relatively free of organic contamination, as oily species were not observed and the particles are distributed on the entire TEM grid, unlike the nanoparticles made from organogermanes at higher temperature, which

(23) Newman, R. C.; Wake-field, J. *Solid State Phys. Electron. Telecommun., Proc. Int. Conf.* **1960**, *1*, 160.
(24) Launay, J. C.; Debegnac, H.; Zappoli, B.; Mignon, C. *J. Cryst. Growth* **1988**, *92*, 323.
(25) Wu, Y.; Yang, P. *Chem. Mater.* **2000**, *12*, 605.
(26) King, R. B. *Inorg. Chem.* **1963**, *2*, 199.

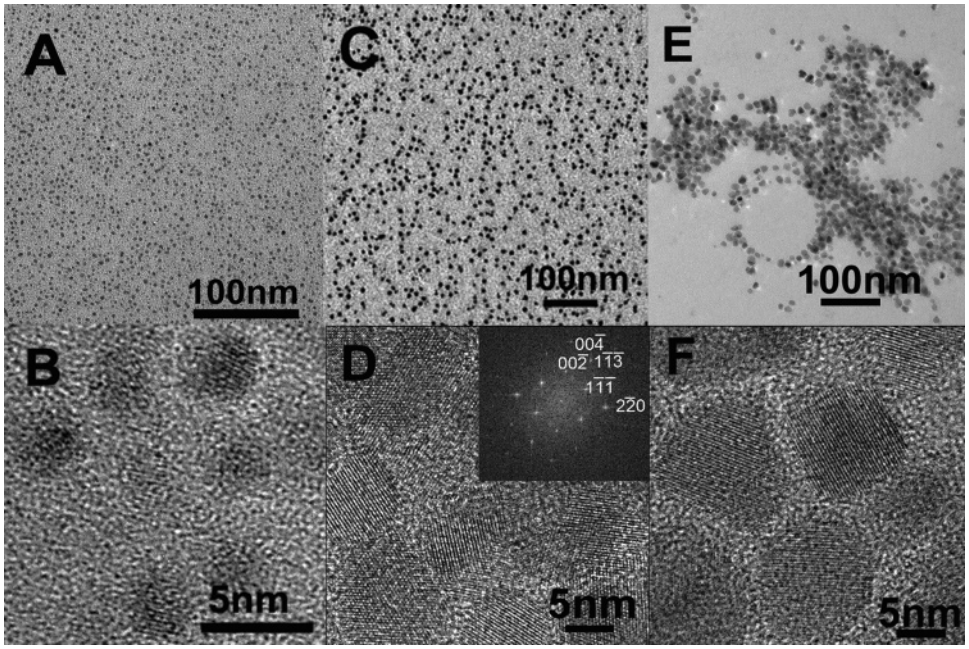

Figure 1. LRTEM and HRTEM images of (A, B) 3.0 ± 0.5, (C, D) 8.1 ± 1.4, and (E, F) 11.6 ± 2.2 nm Ge nanoparticles synthesized from 130, 260, and 520 mM GeI_2 solution in TOP at 300 °C, respectively. HRTEM images show lattice fringes for most of the nanocrystals. The observed lattice spacings of 3.26 and 2.00 Å correspond to the {111} and {220} planes of diamond cubic Ge. (Inset of D) the FFT of a single nanoparticle imaged down the ⟨110⟩ zone axis. A forbidden spot [00$\bar{2}$] appears in the pattern, which can be attributed to double diffraction from [1$\bar{1}$1] and [$\bar{1}$11].

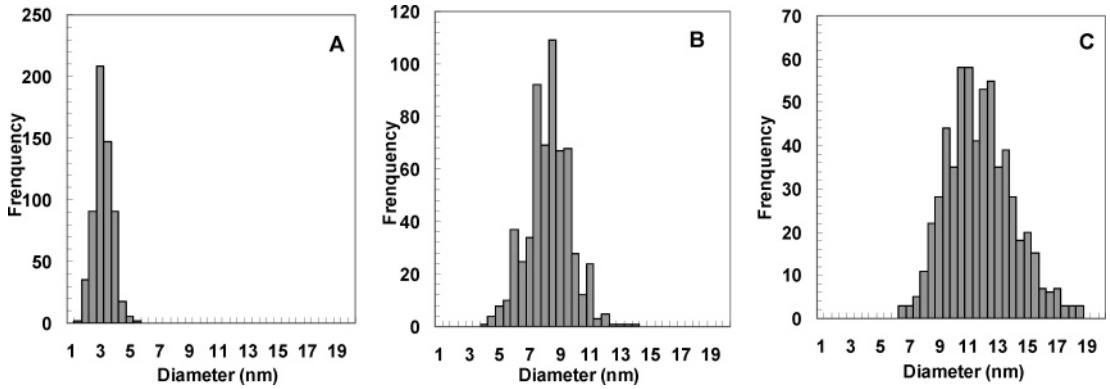

Figure 2. Size distribution for Ge nanoparticles with diameters of (A) 3.0 ± 0.5, (B) 8.1 ± 1.4, and (C) 11.6 ± 2.2 nm.

contained a large amount of organic byproducts even after extensive washing.[18] The average nanocrystal diameters were obtained by counting 600 nanocrystals for each sample with Scion Image software (Scion Co.). A 260 mM amount of GeI_2 in TOP (at 300 °C) gave nanocrystals with an average diameter of 8.1 ± 1.4 nm with 90% of the particles ranging between 6 and 10 nm. The nanocrystal diameter could be varied by changing the GeI_2 concentration. The diameter increased to 11.6 ± 2.2 nm for 520 mM GeI_2 in TOP and decreased to 3.0 ± 0.5 nm when the concentration of GeI_2 in TOP was decreased to 130 mM.

Figure 2 shows the Ge nanocrystal size distributions obtained from reactions with 130, 260, and 520 mM GeI_2 in TOP. The average particle diameter increases from 3.0 to 8.1 to 11.6 nm with the increased precursor concentration. The polydispersity, however, was relatively independent of the precursor concentration with the standard deviations about the mean diameter of 16.7, 17.3, and 19.0%, respectively.

High-resolution TEM of fields of nanocrystals (Figure 1B,D,F) and X-ray diffraction (XRD) (Figure 3) confirmed that the nanocrystals were crystalline with diamond cubic Ge structure. The Ge nanocrystals of different size exhibited primarily single-crystal domains according to the HRTEM images. Figure 1B, for example, shows a field of crystalline 3 nm Ge nanocrystals with 3.26 and 2.00 Å *d* spacings corresponding to the {111} and {220} planes in diamond cubic Ge. An example of a fast Fourier transform (FFT) of an HRTEM image of an individual particle is shown in the inset in Figure 1D. The 9 nm diameter particles show diffraction spots corresponding to *d* spacings of 3.26, 2.00, 1.70, and 1.41 Å, which index to the Ge {111}, {220}, {311}, and {400} cubic phase reflections, respectively. The XRD peaks also match the expected {111}, {220}, and {311} peaks for bulk Ge. The diffraction peak line broadening in the XRD pattern results from the small nanocrystal diameter. From the Scherrer equation, the peak broadening values of 2.58, 1, and 0.78° for the fwhm of the {111} peak of the nanocrystals made from 130, 260, and 520 mM GeI_2 in TOP indicate average diameters of 3.1, 8.0, and 10.3 nm, consistent with the average diameters determined from TEM images of 3.0, 8.1, and 11.6 nm, respectively.

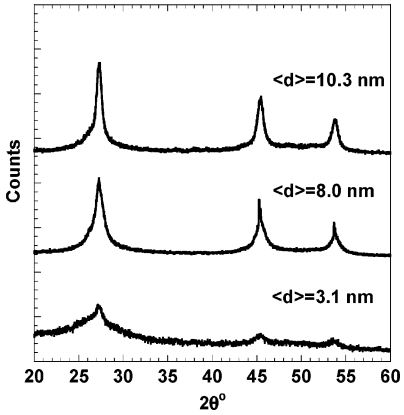

Figure 3. Powder XRD of three different Ge nanocrystal preparations with different average particle diameter. Each sample shows the characteristic {111}, {220}, and {311} diffraction peaks for diamond cubic Ge. Increased peak broadening occurs for the smaller diameter nanocrystals. The full width at half-maximum (fwhm) of the {111} reflection is 2.58, 1.0, and 0.78°, corresponding to Scherrer diameters of 3.1, 8.0, and 10.3 nm, which are consistent with the TEM measurements of 3.0, 8.1, and 11.6 nm, respectively.

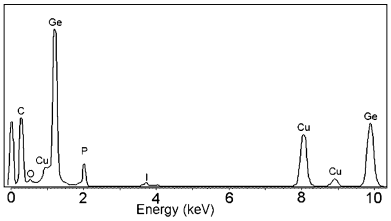

Figure 4. EDS spectrum obtained from the 11.6 nm Ge nanocrystals imaged by TEM in Figure 1E. The peaks at 1.2 and 9.8 keV correspond to the Lα and Kα lines of Ge. The copper and carbon peaks result from the copper TEM grid coated with carbon film.

EDS data (Figure 4) also confirmed the presence of Ge in the sample. In addition to Ge, small amounts of O, P, and I are also observed by EDS. P is most likely from bound TOP and possibly trioctylphosphine oxide (TOPO), O could be from surface oxide or possibly TOPO, and I could be due to adsorbed precursor byproduct. Relative to the Ge signal; however, the intensities of O, P, and I peaks are very low, indicating very small amounts of those species.

The FTIR spectrum in Figure 5 of 8.1 nm diameter Ge nanocrystals reveals three peaks at 2956, 2920, and 2854 cm^{-1} that correspond to C−H stretching modes for CH_2 and CH_3 groups, indicating that hydrocarbon species are present. The peaks at 1463 and 1378 cm^{-1} are also consistent with the CH_3 bending vibrations. The peaks ranging from 700 to 1100 cm^{-1} are very similar to the IR of TOP,[27] consistent with the presence of TOP as a stabilizing ligand. Although FTIR does not provide definitive proof that organic ligands are bonded to the nanocrystal surface, the FTIR spectra are consistent with the presence of a hydrocarbon layer on the particle surface.

XPS was used to probe the extent of Ge nanocrystal surface oxidation. Like silicon, Ge is highly sensitive to oxidation. Various organic species have been studied as surface passivants for Ge that prevent or slow significantly surface oxidation, including alkenes, thiols, and alkynes.[28,29] We are not aware of any studies that have examined TOP as a passivating ligand for Ge surfaces. XPS data were obtained from Ge nanocrystals drop cast from chloroform onto oxidized silicon substrates. Ge has signature peaks at

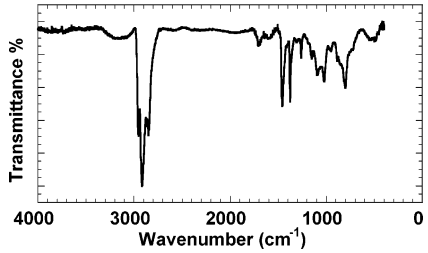

Figure 5. FTIR spectra of 8.1 nm Ge nanocrystals made from 260 mM GeI_2 in TOP at 300 °C.

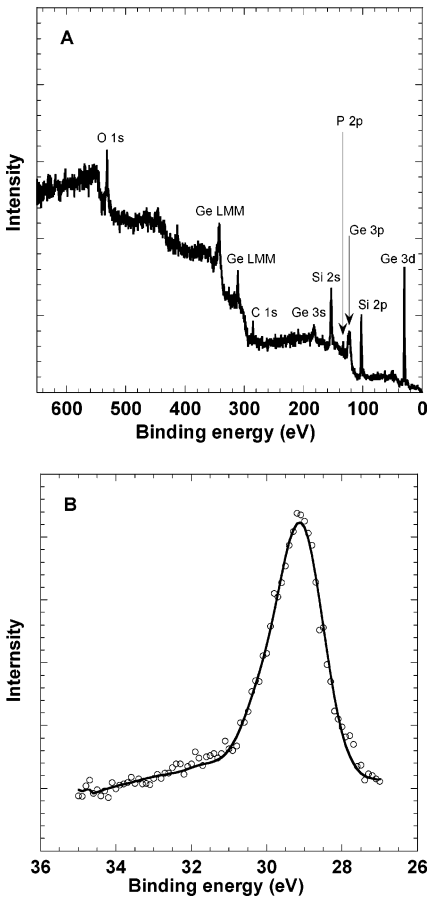

Figure 6. XPS spectra of 8.1 nm Ge nanocrystals. (A) Survey scan of the sample on Si substrate, the peaks of Si and O are from the substrate with an oxidation layer. (B) High-resolution Ge 3d scan.

29.0 and 29.6 eV, attributed to $3d_{5/2}$ and $3d_{3/2}$, respectively.[30] Ge oxidation gives rise to satellite peaks associated with Ge^{1+}, Ge^{2+}, Ge^{3+}, and Ge^{4+} oxidation states, each with an associated energy shift of 0.8, 1.8, 2.6, and 3.4 eV relative to the binding energy of 29.0 eV for Ge $3d_{5/2}$, respectively.[31] The native oxide of Ge, GeO_2, has a photoelectron peak maximum of 32.4 eV.[30] A low-resolution scan for 8.1 nm Ge nanocrystals made from 260 mM GeI_2 in TOP at 300 °C (Figure 6A) shows Ge 3d (29 eV), 3p (123 eV), and 3s (183 eV) and Ge LMM (311, 342 eV) peaks. Peaks at 130 and 285 eV correspond to P 2p and C 1s, indicating the presence of alkylphosphines in the sample, which serve as the

(27) Pouchert, C. J. *The Aldrich Library of FT-IR spectra*, 2nd ed.; Aldrich: Milwaukee, WI, 1997.
(28) Hanrath, T.; Korgel, B. A. *J. Am. Chem. Soc.* **2004**, *126*, 15466.
(29) Choi, K.; Buriak, J. M. *Langmuir* **2000**, *16*, 7737.
(30) Oh, J.; Campbell, J. C. *J. Electron. Mater.* **2004**, *33*, 364.
(31) Schmeisser, D.; Schnell, R. D.; Bogen, A.; Himpsel, F. J.; Rieger, D.; Landgren, G.; Morar, J. F. *Surf. Sci.* **1986**, *172*, 455−465.

Table 1. Summary of Synthetic Approaches for Production of Ge Nanocrystals in Solution[a]

Ge precursor	reducing agent	temp	stabilizer	solvent	ref
$GeCl_4$	NaK alloy	270 °C	$RMCl_3$ (M = Si/Ge)	heptane	9
$GeCl_4$	$Li[C_{10}H_8]$	room temp	CH_3SiCl	tetrahydrofuran	10
GeX_4[b]	$LiAlH_4$	room temp	micelle	octane	11
$GeCl_4$	NaGe/KGe/Mg_2Ge		glyme/diglyme	glyme/diglyme	12−15
GeI_4	$LiAlH_4$		*n*-alkene	tetrahydrofuran	16
TEG[b]	thermal reduction	400 °C	organic molecules	hexane	17
TEG/DPG[b]	thermal reduction	400−500 °C	octanol	hexane	18−1 9
TEG/DPG[b]	thermal reduction	500 °C	octanol	supercritical CO_2	20
$Ge[N(SiMe_3)_2]_2$	thermal reduction	300 °C	oleylamine	octadecene	21
GeI_2	$LiAlH_4$	300 °C	TOP	TOP	this study

[a] Only refs 14, 21, 22, and this study report yields. [b] X = Cl,Br or I; TEG = tetraethylgermane; DPG = diphenylgermane.

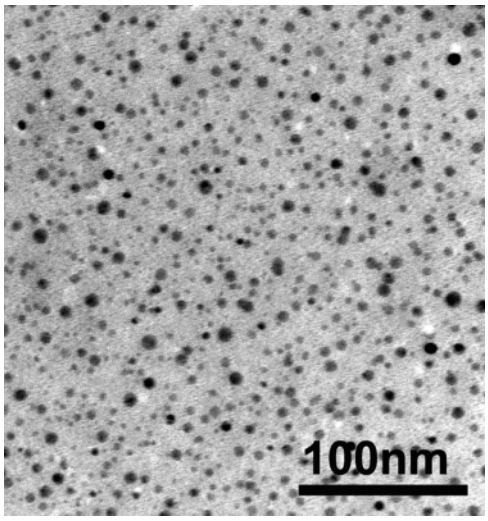

Figure 7. LRTEM of Ge nanocrystals with a diameter of 6.4 ± 3.5 nm made from a 130 mM solution of GeI_2 in TBP at 240 °C.

nanocrystal capping ligands in the synthesis. The absence of peaks from Al (2p 73 eV), I (3d 619 eV), and Li (1s, 55 eV) confirms minimal contamination from those species. Figure 6B shows a higher resolution XPS scan of the 3d Ge peak. Although the splitting of Ge 3d to $3d_{5/2}$ and $3d_{3/2}$ was not well resolved, the peak centered at 29.2 eV was in good agreement with the expected value for elemental Ge. Barely noticeable photoelectron signals between 30.4 and 34.0 eV were observed, indicating that minimal surface oxidation occurs during the purification process.

Nanocrystal Synthesis in TBP. TBP was also used as a coordinating solvent for synthesis of Ge nanocrystals from GeI_2. The reaction was carried out in TBP at lower temperature (240 °C) due to its lower boiling point relative to TOP. Figure 7 shows a TEM image of Ge nanoparticles made from 130 mM GeI_2 in TBP with 65 mM $LiAlH_4$. The particles had an average diameter of 6.4 nm with a standard deviation of 55%. Compared to reactions in TOP with the same GeI_2 concentration, the Ge nanoparticles made in TBP exhibit larger average diameter (6.4 nm vs 3.1 nm) with a broader size distribution (55% vs 17%). This difference suggests that the higher steric barrier provided by the longer TOP alkyl chains offers better size control for Ge nanocrystals, similar to the case of CdSe nanoparticles synthesized in TBP and TOP.[6]

Discussion

Ge Precursor Chemistry. $LiAlH_4$ reduction of GeI_2 in TOP at 300 °C gives high chemical yields of Ge nanocrystals. To put these results in perspective, we have summarized in Table 1 other solution-phase synthetic methods for Ge nanocrystals from the literature. Compared to the widely used Ge(IV) precursors, GeX_4 (X = Cl, Br, and I) and organogermanes, GeI_2 offers various advantages. First, the formation of the complex (GeI_2)·TOP makes GeI_2 highly soluble in TOP, up to a concentration of 0.5 M GeI_2 at room temperature. In contrast, the solubility of GeI_4 in hydrocarbon solvents is fairly low. The high Ge precursor concentration produces a large supersaturation of Ge atoms in the initial stages of the reaction to produce a high particle nucleation rate. The high nucleation rate is desirable for the potential formation of small crystals with low polydispersity. Second, the high boiling point of GeI_2 facilitates reactions at ambient pressure even at high temperatures, which favors the formation of elemental Ge. Attempts have been tried by many research groups to make Ge nanoparticles by reduction of $GeCl_4$ with $LiAlH_4$. However, the low boiling point of $GeCl_4$ (83 °C) limits the reaction temperature under atmospheric pressure, and the highly corrosive byproducts (e.g. HCl) can be undesirable. Most significantly, $LiAlH_4$ reduction of $GeCl_4$ at low temperature (<80 °C) yields mostly GeH_4 and oligomeric germanes of Ge_xH_{2x+2} (such as Ge_5H_{12}, Ge_7H_{16}, etc.), instead of Ge,[32,33] which can limit the Ge nanocrystal yield significantly. Although reduction of GeI_2 with $LiAlH_4$ may also form Ge_xH_{2x+2} species, they will decompose to elemental Ge and hydrogen at the higher reaction temperature (~300 °C).[32] GeI_2 is also easier to reduce to Ge than GeX_4. At 25 °C, the reduction potential of Ge(II) to Ge(0) is greater than that of Ge(IV) to Ge(0) (0.247 vs 0.124 eV).[21,3434] Furthermore, GeI_2 disproportionates to Ge and GeI_4 even without the presence of reducing agent at ~330 °C. This high reactivity of GeI_2 enables a high chemical yield of Ge nanocrystals.

Although the reaction mechanism for reduction of GeI_2 by $LiAlH_4$ in the presence of alkylphosphines is not fully characterized, the following possible reactions are likely present: GeI_2 disproportionation to GeI_4 and Ge; GeI_2 reduction to Ge by $LiAlH_4$; and GeI_4 reduction to Ge or Ge(II) by $LiAlH_4$. The major byproducts of those reactions are iodides, including LiI and AlI_3. EDS of the Ge nanocrystal product revealed only a limited presence of I, indicating that most of the iodide contaminants are removed in the purification step as expected: LiI is soluble in acetone,

(32) Stone, F. G. A. *Hydrogen Compounds of Ground IV Elements*; Prentice Hall: Englewood Cliffs, NJ, 1962.
(33) Macklen, E. D. *J. Chem. Soc.* **1959**, 1984.
(34) Galus, Z. *Stand. Potentials Aqueous Solution* **1985**, 189.

and AlI_3 is not soluble in chloroform.

Approaches to control the Ge nanocrystal size include inverse micelles as templates[11,22] and covalent bonding of hydrocarbons with reactive functional groups.[12,17,18] In the latter case, the possibility of forming long-chain Ge compounds with polymerized hydrocarbon groups at high reaction temperature (>400 °C) may in part account for the low yield of nanoparticles. In addition, hydrocarbon decomposition can occur at these temperatures, leading to oligomeric byproducts that can be very difficult to separate from the nanocrystals. An alternative approach is to minimize hydrocarbon decomposition byproducts by synthesizing Ge at 500 °C in the chemically inert solvent, supercritical CO_2, which is capable of solvating octanol as a capping ligand at this high temperature.[20] However, the particle sizes were significantly larger than in the present study.

Although TOP is one of the most commonly used coordinating solvents in the synthesis of colloidal Group II−VI semiconductor nanocrystals (e.g. CdSe[6]), this is the first report where it has been employed as a solvent to synthesize Ge nanoparticles. Since the reduction of GeI_2 with $LiAlH_4$ was conducted at a mild temperature (∼300 °C), the formation of hydrocarbon free radicals, which would lower the yield of nanoparticles by competing with Ge homogeneous nucleation to form organogermane oligomers, was minimized if not completely avoided. The mechanism for the passivation of the particles in this study is unknown but would be influenced by the known coordination of TOP with GeI_2 to form the (GeI_2)·TOP complex during reaction.[32]

Ge Nanocrystal Growth. Colloidal nanocrystal formation involves two steps: nucleation, which relieves the excess free energy of the supersaturated solution, followed by particle growth. To achieve monodisperse size distributions, the nucleation and growth steps must be temporally separated to ensure that new nuclei are not forming during the growth stage.[35−37] Once nucleated, the particles may grow by either (1) reactant diffusion-limited growth with Ge atom condensation on existing particles or (2) aggregation of existing particles. To determine which of these growth mechanisms is dominant in Ge nanocrystal synthesis, a similarity transformation technique was used to analyze the moments of the size distribution of the nanoparticles. This analysis of particle size distributions, developed by Friedlander et al.[38,39] to study the growth mechanism of aerosol particles, was extended recently by Shah et al.[40] to analyze the growth mechanism of colloidally grown silver nanocrystals in supercritical carbon dioxide. At relatively long times after particle nucleation, the size distribution becomes independent of the initial nucleation event and will reflect the particle growth mechanism. The two growth mechanisms of condensation and aggregation may be in competition, with condensation narrowing the size distribution at long times and aggregation broadening it.[41] The extent to which aggregation and condensation control particle growth can be determined by examining the moments of the size distribution function $\mu_1 = r_3/r_h$ and $\mu_3 = r_1/r_3$, where r_1 is the arithmetic mean radius defined as $r_1 = \sum r_i/N_\infty$; r_3 is the cubic mean radius defined as $r_3 = (\sum r_1^3/N_\infty)^{1/3}$; and r_h is the harmonic mean radius defined as $r_h = N_\infty/(\sum 1/r_i)$. For a monodisperse sample, $r_1 = r_3 = r_h$ and $\mu_1 = \mu_3 = 1$. Significant deviations from 1, with $\mu_1 > 1.25$ and $\mu_3 < 0.905$, indicate that particles grow primarily by aggregation.

Table 2. Calculated Moments of the Size Distribution for Ge Nanocrystals Synthesized in TOP

particle diameter (nm)	μ_1	μ_3
3.0	1.09	0.96
8.1	1.07	0.97
11.6	1.08	0.96

For the analysis, the total number of particles N_∞, were obtained by integrating the experimental size distributions determined by TEM, as a function of particle volume (i.e., $v_i = (4/3)\pi r_i^3$):

$$N_\infty = \int_0^\infty n(v)\, dv \qquad (1)$$

$n(v)$ is the number concentration of particles with volume between v and $v + dv$. Table 2 summarizes the calculated values of μ_1 and μ_3 of the Ge nanocrystals. For the three different nanocrystal preparations, both μ_1 and μ_3 are close to unity, indicating that the nanocrystals grow primarily by condensation (Table 2). The high concentration of passivating ligand TOP limits particle aggregation, as well as other factors in the reaction mechanism that favor growth by condensation. Upon the rapid introduction of $LiAlH_4$ into the GeI_2 solution at 120 °C, germanes Ge_xH_{2x+2} and high supersaturation of elemental Ge are formed to produce rapid nucleation rates. With increasing temperature, more Ge atoms are supplied to the nuclei by decomposition of Ge_xH_{2x+2}, which sustains the growth of the nanoparticles by condensation.

Conclusions

High chemical yields up to 73% (moles of recovered Ge per mole of initial GeI_2, without including the weight of the capping ligands) of Ge nanocrystals, with sizes ranging from 3 to 11 nm, have been synthesized by reducing GeI_2 with $LiAlH_4$ in TOP at 300 °C and in TBP at 240 °C. The weight of ligands on the surface was unknown, but a full monolayer would change the total weight by less than 10% based on the short length of the ligands. The particle size increased monotonically with increased GeI_2 precursor concentration. High-quality Ge nanocrystals in 95 mg quantities were obtained, and the simple batch process is suitable for scaleup to produce larger quantities. The high yield is due to a combination of advantages compared with previous syntheses, including the higher reactivity of Ge(II) versus Ge(IV), high solubility of (GeI_2)·R_3P complexes, the lower concen-

(35) Murray, C. B.; Kagan, C. R.; Bawendi, M. G. *Annu. Rev. Mater. Sci.* **2000**, *30*, 545.
(36) Burda, C.; Chen, X. B.; Narayanan, R.; El-Sayed, M. A. *Chem. Rev.* **2005**, *105*, 1025.
(37) Yu, W. W.; Falkner, J. C.; Shih, B. S.; Colvin, V. L. *Chem. Mater.* **2004**, *16*, 3318.
(38) Swift, D. L.; Friedlander, S. K. *J. Colloid Sci.* **1964**, *19*, 621.
(39) Friedlander, S. K.; Wang, C. S. *J. Colloid Interface Sci.* **1966**, *22*, 126.
(40) Shah, P. S.; Husain, S.; Johnston, K. P.; Korgel, B. A. *J. Phys. Chem. B* **2001**, *105*, 9433.
(41) Watzky, M. A.; Finke, R. G. *J. Am. Chem. Soc.* **1997**, *119*, 10382.

tration of byproducts and solvent degradation due to moderate temperatures, the lack of organic impurity atoms in the precursor, and passivation of the surface with TOP ligands. Reaction in TBP produced larger nanoparticles with much broader size distribution than TOP for a given concentration of GeI_2, presumably due to weaker steric stabilization by the shorter alkyl chain of TBP. The moments of the size distribution of the Ge nanoparticles synthesized in TOP indicate condensation-controlled growth. This result is consistent with the observation of single crystals by HRTEM and XRD and the moderate polydispersity. FTIR and XPS spectra of the nanoparticles showed the presence of hydrocarbon groups and the limited oxidation of the particles. Together, these results indicated that the TOP and TBP coated the surfaces of the particles to provide passivation against coagulation and oxidation.

Acknowledgment. This material is based upon work supported in part by the Department of Energy Office of Basic Energy Sciences (Grant DE-FG02-04ER15549), the Robert A. Welch Foundation, the National Science Foundation, the Advanced Materials Research Center (AMRC) in collaboration with International SEMATECH, and the Separations Research Program at the University of Texas. The authors also thank John Ekerdt, Damian Aherne, David Jurbergs, Fred Mikulec, and Susan Kauzlarich for insightful discussions and J. P. Zhou for assistance with HRTEM imaging.

CM0515956